Polymer Bulletin (2019) 76:3957–3970
https://doi.org/10.1007/s00289-018-2581-x

ORIGINAL PAPER

Dielectric properties and thermal conductivity of epoxy resin composite modified by Zn/ZnO/Al_2O_3 core–shell particles

Yang Wang[1] · Lingjie Zhu[1] · Jun Zhou[1] · Beibei Jia[1] · Yingye Jiang[1] · Junkai Wang[1] · Menglan Wang[1] · Yonghong Cheng[1] · Kai Wu[1]

Received: 1 June 2018 / Revised: 10 September 2018 / Accepted: 21 October 2018 /
Published online: 31 October 2018

Abstract

Herein, the effect of multilayer core–shell-structured Zn/ZnO/Al_2O_3 particles on thermal conductivity and dielectric properties of epoxy composites was investigated. The core–shell-structured Zn/ZnO particles were obtained by a simple calcination method, and the multilayer core–shell-structured Zn/ZnO/Al_2O_3 particles were prepared using hydrolysis process. The Zn/ZnO/Al_2O_3/epoxy composites were fabricated, and atomic force microscopy (AFM) images showed that the fillers were well distributed in epoxy matrix. Thermal conductivity of Zn/ZnO/Al_2O_3/epoxy composites increased 178% by adding 12.0 wt% of Zn/ZnO/Al_2O_3 particles. The dielectric constant of composites increased obviously with the increased content of Zn/ZnO/Al_2O_3 particles, while the dielectric loss is still low. These results illustrate that the combination of the thermal and dielectric properties tuned by multilayer core–shell particles gives potential application in extended domains for epoxy composites.

Keywords Epoxy composites · Core–shell particles · Packaging materials · Thermal conductivity · Dielectric constant

Introduction

The multiple properties of polymer-based materials have attracted a great attention due to a lot of applications. Epoxy resin (ER), as one of the important polymers, is widely used in insulation such as electrical engineering, power electrical equipments and packing of integrated circuits [1]. Thermal management is critical to the performance, lifetime and reliability of electronic devices. With the miniaturization, integration and functionalization of electronics and the emergence of new applications such as light-emitting

✉ Jun Zhou
zhoujun@mail.xjtu.edu.cn

[1] Center of Nanomaterials for Renewable Energy, State Key Laboratory of Electrical Insulation and Power Equipment, Xi'an Jiaotong University, Xi'an 710049, People's Republic of China

diodes, thermal dissipation becomes a challenging problem [2–4]. Moreover, for some specific applications, the dielectric properties and thermal conductivity need to be improved. Thus, the inorganic fillers with high dielectric constant (high-*k*) were usually added into the epoxy matrix to reach proper properties, and the designed composites are then formed. These polymeric composites are considered as heterogeneous disordered systems [5]. Their performances depend on many factors, such as electrical properties of their constituents, geometric characteristics, volume fraction of the filler and the spatial distribution of the fillers within the polymeric matrix [6–12]. High loading (> 50 vol%) of the inorganic fillers in the polymeric materials can increase *k* dramatically; however, the dielectric loss (tan δ) also increases rapidly. On the other hand, interactions between fillers and matrix can also influence the dielectric properties of such composites.

Nowadays, the core–shell-structured inorganic powders, especially the metal–insulator particles, have been employed to prepare composites with high dielectric constant and low loss. In this case, the metal core is meant to increase the dielectric constant ascribed to the interfacial polarization, while the insulator shell is used to control the dielectric loss effectively by blocking the electron transfer between back-fence metal cores [13]. Generally, the core–shell-structured particles were prepared by chemical syntheses, and most of them are complicated and inefficient. The core–shell Ag/C particles were synthesized via a hydrothermal method and served as special fillers to enhance the dielectric constant [9]. Dang et al. [14] reported that Ag/TiO_2 core–shell-structured particles can remarkably increase the dielectric constant of polymer composites. The core–shell-structured Fe/FeO nanoparticles were also embedded in epoxy resins to improve the thermal stability and introduce magnetic properties [15]. Zhang and co-workers [6] synthesized Zn/ZnO particles using the heat treatment of raw Zn particles under air, and they found that the dielectric constant of Zn–ZnO/PVDF composites enhanced dramatically, while the dielectric loss was still low. However, it remains a challenge to enhance the dielectric constant and thermal conductivity of thermosetting polymers simultaneously.

In this work, the multilayer core–shell-structured Zn/ZnO/Al_2O_3 particles are used as fillers to tune the physical properties of epoxy resins. The inner core–shell Zn/ZnO particles are prepared by a simple heat treatment of Zn metal particles in ambient air. The detailed structure and morphology in the different heat treatment conditions for Zn metal particles were investigated by XRD and SEM. Then, Al_2O_3 layers were coated on the surface of Zn/ZnO particles by a simple chemical process. The fracture microstructure of the composites is evaluated by a scanning electron microscope (SEM). Atomic force microscopic (AFM) is also used to inspect the distribution of the particles in epoxy resins. The thermal conductivity of the composites is evaluated, and the dielectric properties are also examined by an impedance analyzer.

Experimental

Sample preparation

Raw Zn metal particles were heated in a tube furnace under air at 400–500 °C for 2–4 h. A thin layer of ZnO was formed on the surface of Zn metallic core, and the

core–shell-structured Zn/ZnO particles were obtained. This process is similar to the previous work [6]. Then, the multilayer core–shell-structured Zn/ZnO/Al_2O_3 particles were prepared by coating the surface of Zn/ZnO microsphere with Al_2O_3 obtained from hydrolysis of aluminum sulfate [$A1_2(SO_4)_3$]. Firstly, the suspension of Zn/ZnO was prepared by means of ultrasonic dispersion for 1 h. After increasing the temperature of the suspension up to 80 °C, the proper amount of $A1_2(SO_4)_3$ was added into the solution and the PH value was adjusted to 8.5–11. The core–shell-structured Zn/ZnO/Al_2O_3 particles were obtained by centrifugation and washed several times with water and ethanol, and then dried at 80 °C for 4 h.

The core–shell-structured Zn/ZnO and Zn/ZnO/Al_2O_3 particles were separately dispersed into bisphenol A-based epoxy resins (ER, Wenzhou Gaodesheng Insulating Materials Co., Ltd.) and sonicated for 30 min. 2,2-Bis-(4-cyanatophenyl) propane (CE, Zhejiang Shangyu Chemical Co., Ltd.) was heated at 160 °C for 15 min with vigorous stirring. The temperature was decreased to 100 °C. Then, the mixtures were mixed with CE, and the whole system was stirred for 0.5 h to form a homogeneous liquid. A preheated mold with silicon coating on the inner surface was heated at 120 °C for 1 h. The as-prepared mixture was poured into the preheated mold. The mixture was degassed at 60 °C for 0.5 h in a vacuum oven to remove the bubbles. Finally, the polymeric mixture was cured by the following procedure: 100 °C/2 h, and post-cured at 150 °C/10 h.

Characterization techniques

The particle size and morphology were visualized by using a FEI Quanta 600 FEG scanning electronic microscope (SEM) and a FEI Tecnai G2 F20 S-TWIN transmission electron microscope (TEM). Energy-dispersive X-ray spectrometry (EDX) was used to perform EDX spectra of the powders. The morphologies of core–shell microspheres in composite films were examined by atomic force microscope (AFM, Bruker Dimension Icon; operated in the PeakForce QNM mode at 0.8 Hz scanning rate). Platinum–iridium-coated probes (SCM-PIT, Bruker) were used in the AFM measurements. The thermal diffusivity (δ) and specific heat (C) were measured on disk samples by using a LFA447 light flash system (NETZSCH, Selb, Germany) at 25 °C. The bulk density (ρ) of the specimen was measured by water displacement. The thermal conductivity (λ, W m^{-1} K^{-1}) was given by the product of the thermal diffusivity (δ, mm^2 s^{-1}), specific heat (C, J g^{-1} K^{-1}) and bulk density (ρ, g cm^{-3}):

$$\lambda = \delta \cdot C \cdot \rho$$

The broadband frequency dielectric properties of the composites were measured using a Concept 80 impedance analyzer (Novocontrol, Germany) over the frequency range of 10^{-1} to 10^6 Hz. All samples were prepared by fracturing the composites at liquid nitrogen temperature and then sputter coating them with a homogeneous gold layer to avoid accumulation of charges.

Results and discussion

Preparation of core–shell-structured Zn/ZnO and Zn/ZnO/Al_2O_3 particles

After being exposed to oxidized atmosphere, ZnO layer is easily formed on the surface of metallic Zn particle and the thickness of ZnO layer could be adjusted if the calcined temperatures are controlled. Zhang and co-workers [6] synthesized Zn/ZnO particles using the heat treatment of raw Zn particles under air at different temperatures; however, no detailed morphology of the particles was given in their work. Generally, the surface property and morphology of fillers are vital for the physical properties of composite polymers. Herein, SEM images of the Zn particles calcined at different conditions are shown in Fig. 1. The raw Zn particles showed smooth spheres, and the diameter is around 2–8 μm (Fig. 1a, b). After being calcined at 400 °C for 2 h, the particles' surface was not smoothed anymore and uneven solids were observed (Fig. 1c, d). The amount of uneven solids increased, while the morphology of particles still maintains uniform spheres when the heating time increased up to 3 h (Fig. 1e, f) and 4 h (Fig. 1g, h). However, the shape of particles became non-uniform after increasing the heating temperature (> 450 °C). In order to prepare the uniform particles, it means that the optimum heating temperature for the formation of core–shell-structured Zn/ZnO is around 400 °C. Thus, the Zn/ZnO particles prepared at 400 °C for 4 h were selected for further study in this work.

Figure 2 shows the XRD patterns of Zn particles after calcination at different conditions. The peaks of ZnO were observed when Zn particles were calcined in air. It confirms that the ZnO layer had formed on the surface of Zn particles. From the EDX spectra of Zn/ZnO/Al_2O_3 powders in Fig. 3, it obviously demonstrates that the elements of Zn, Al, and O were contained in the sample. Figure 4 shows the XRD patterns of the core–shell-structured Zn/ZnO and Zn/ZnO/Al_2O_3 powders. The XRD peaks of Al_2O_3 were present, illustrating that the Al_2O_3 layer was successfully deposited on the surface of Zn/ZnO particles. Figure 5 shows SEM (Fig. 5a) and TEM (Fig. 5b–d) images of Zn/ZnO/Al_2O_3 particles, and the surface of Zn/ZnO particles became rough obviously after Al_2O_3 deposited. Compared to the FTIR curves of Zn/ZnO particles, Zn/ZnO/Al_2O_3 particles presented several additional absorption peaks in the range of 1000–1500 cm^{-1} (as shown in Fig. 6), which are ascribed to the characteristic absorption band of Al_2O_3. This result confirmed that the multilayer core–shell-structured Zn/ZnO/Al_2O_3 particles were synthesized successfully.

Thermogravimetric analysis

As fillers, Zn/ZnO and Zn/ZnO/Al_2O_3 particles were embedded in the epoxy matrix to fabricate composites films, respectively. Figure 7 shows the TGA curves of Zn/ZnO/epoxy composites and Zn/ZnO/Al_2O_3/epoxy composites as a function of the content of fillers. Both pure epoxy and composites are observed to have similar decomposition behavior and the main degradation occurring in one stage. In these curves, the degradation started at the temperature range from 300 to 600 °C. The thermal stability of composites depicts to slightly decrease with

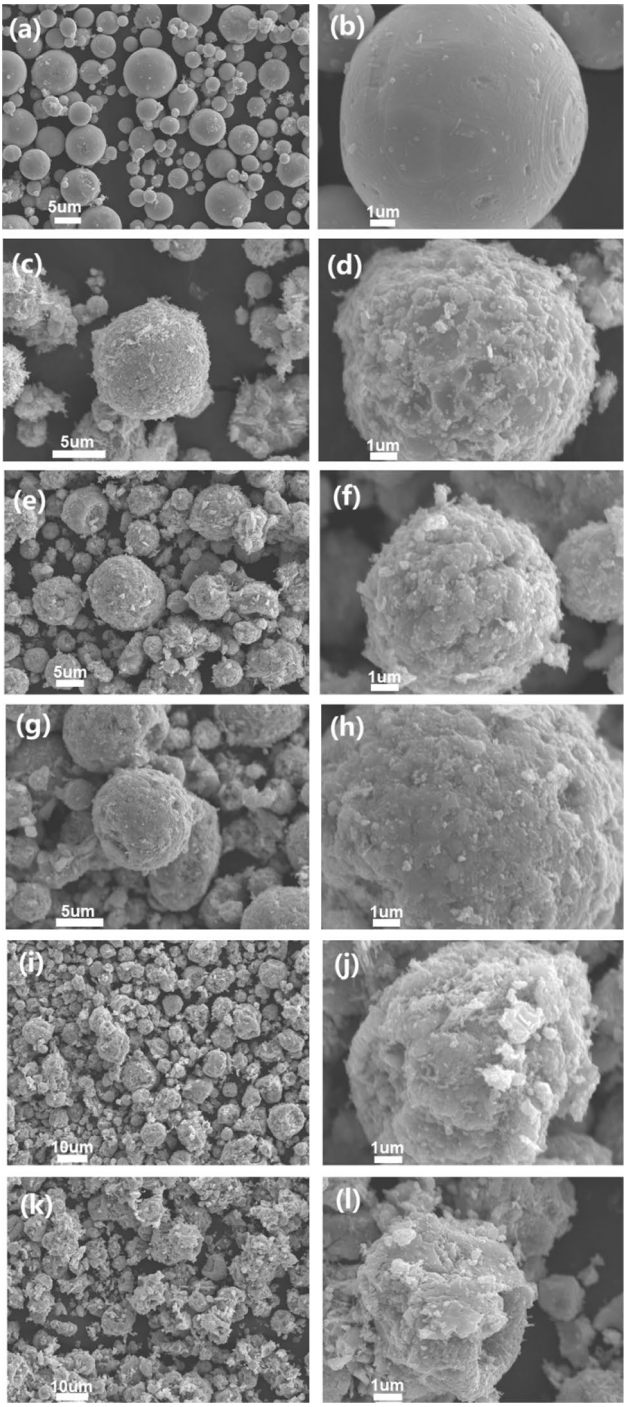

Fig. 1 SEM images of Zn particles treated in air at different conditions. **a**, **b** Unprocessed, **c**, **d** 400 °C + 2 h, **e**, **f** 400 °C + 3 h, **g**, **h** 400 °C + 4 h, **i**, **j** 450 °C + 2 h and **k**, **l** 500 °C + 2 h

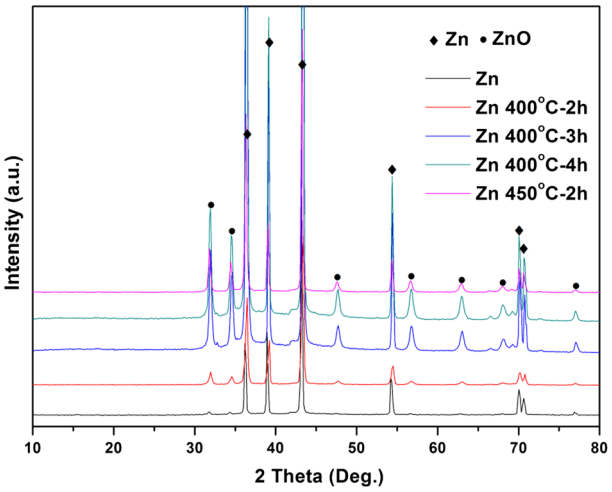

Fig. 2 XRD patterns of Zn particles treated in air at different conditions

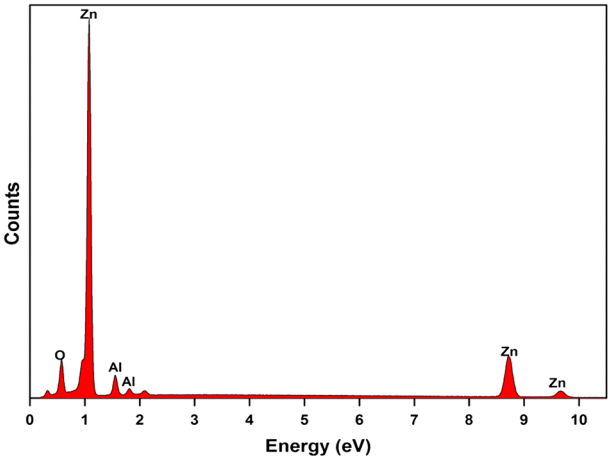

Fig. 3 EDX map of Zn/ZnO/Al_2O_3 particles

the increase in fillers. This may result from the spatial obstruction of particles on the formation of high cross-linked molecular structure of epoxy or increased free volume fractions in the polymer composites [16, 17].

Morphology investigation of epoxy composite films

Figure 8 shows the SEM images of the fracture surfaces of both pure epoxy and composites with different loadings of multilayer core–shell-structured Zn/ZnO/

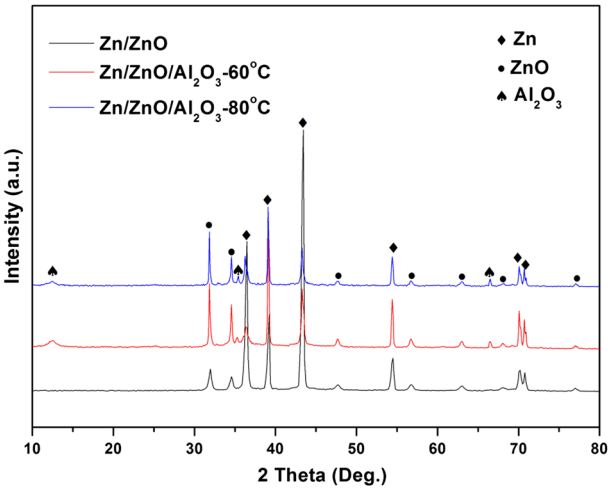

Fig. 4 XRD patterns of Zn, Zn/ZnO and Zn/ZnO/Al_2O_3 particles treated at different temperatures

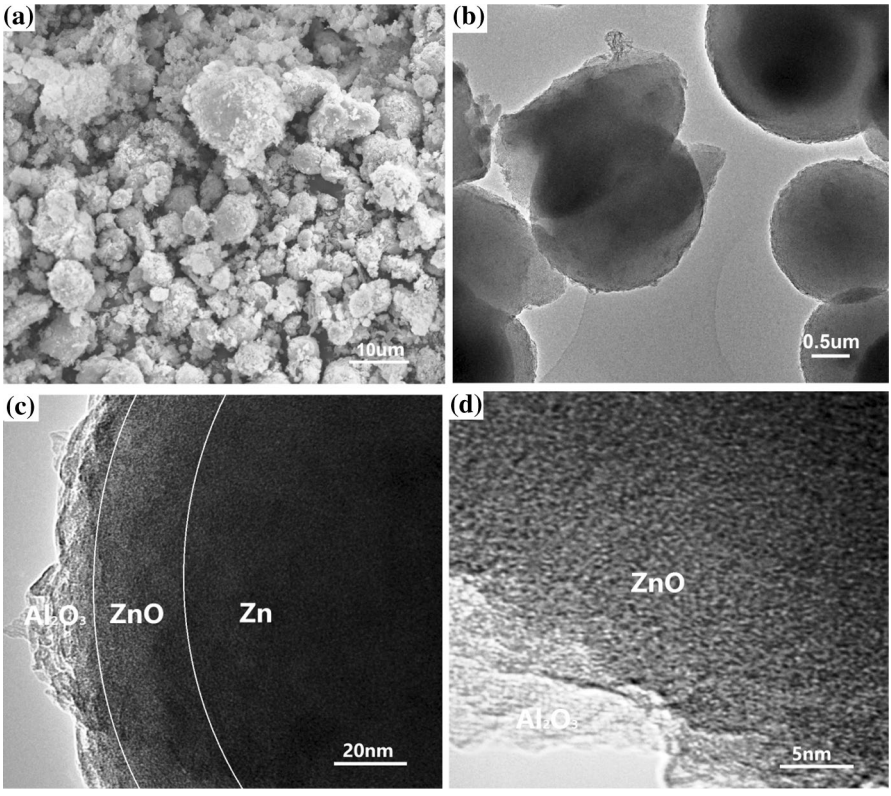

Fig. 5 SEM (**a**) and TEM (**b**–**d**) images of Zn/ZnO/Al_2O_3 particles

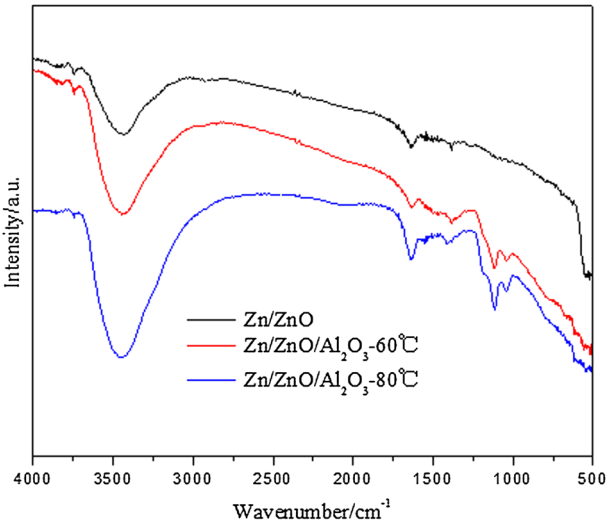

Fig. 6 FTIR of Zn/ZnO and Zn/ZnO/Al_2O_3 particles treated at different temperatures

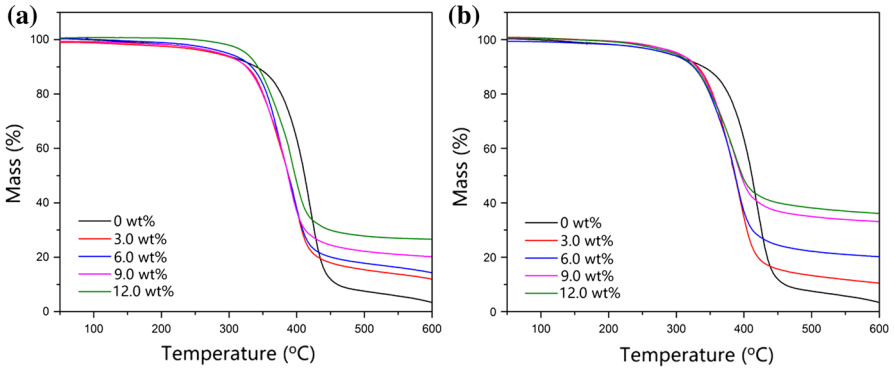

Fig. 7 TGA of Zn/ZnO/epoxy (**a**) and Zn/ZnO/Al_2O_3/epoxy composites (**b**)

Al_2O_3 powders. The cured pure epoxy shows a smooth fracture surface, while the composites show a rough fracture surface, as shown in Fig. 8b–e. Moreover, it can be observed that the core–shell-structured particles are embedded in the epoxy matrix. AFM studies were used to investigate the distribution of fillers in composites. In this work, PeakForce QNM modes have enabled the mapping of the regular height and the adhesion with high spatial resolution simultaneously. Figure 9a, b shows the height image and the adhesion image of Zn/ZnO/Al_2O_3/epoxy composite with the 3.0 wt% core–shell-structured fillers, respectively. From the figures, the embedded Zn/ZnO/Al_2O_3 particles are homogenously distributed within the epoxy matrix, and no obvious aggregation of the Zn/ZnO/Al_2O_3 particles in the composite

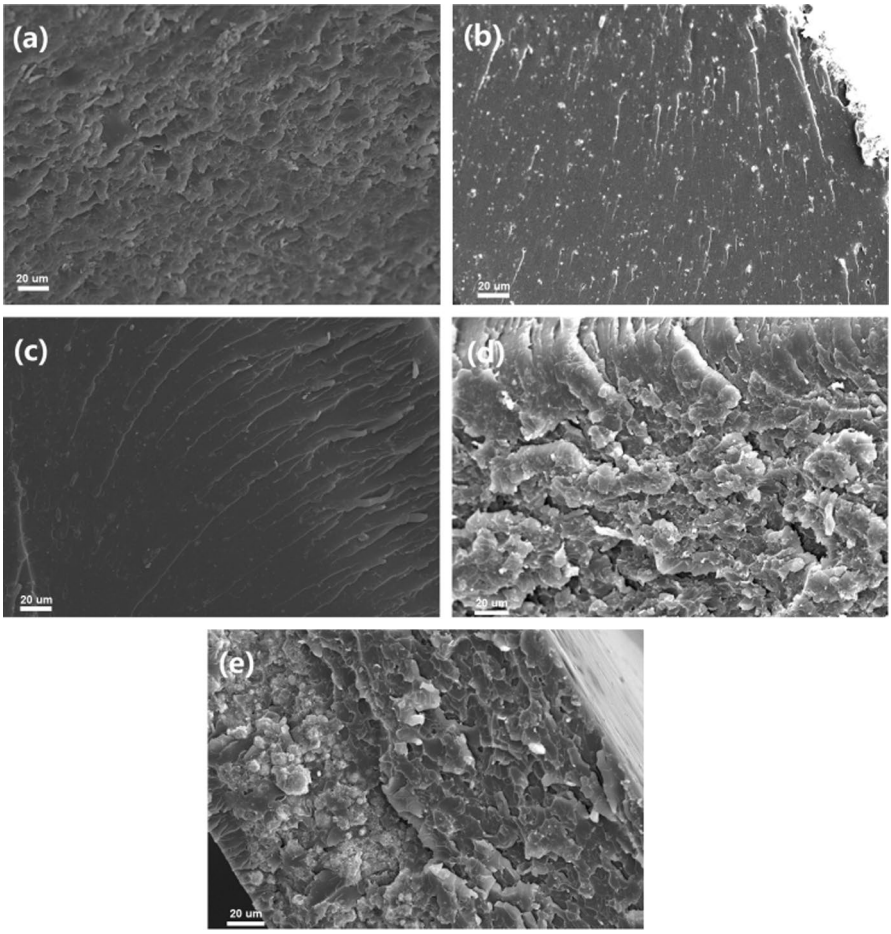

Fig. 8 SEM images of different contents (x) of Zn/ZnO/Al_2O_3 in epoxy composites: **a** $x=0$, **b** 3.0 wt%, **c** $x=6.0$ wt%, **d** $x=9.0$ wt% and **e** $x=12$ wt%

film was found. Figure 9c, d shows that the 3D images of a Zn/ZnO/Al_2O_3 particle were vividly observed and that the particle was embedded in the epoxy matrix.

Thermal conductivity and dielectric properties of epoxy composites

Generally, there are two ways for heat transfer in solids: charge carriers (such as electrons and holes) and phonons (energy quanta of atomic lattice vibrations), respectively [2]. For most polymers, the primary mechanism of heat conduction is by phonons [18]. The thermal conductivity of polymers can be obtained from the following Debye equation:

$$k = \frac{C_p v l}{3} \tag{1}$$

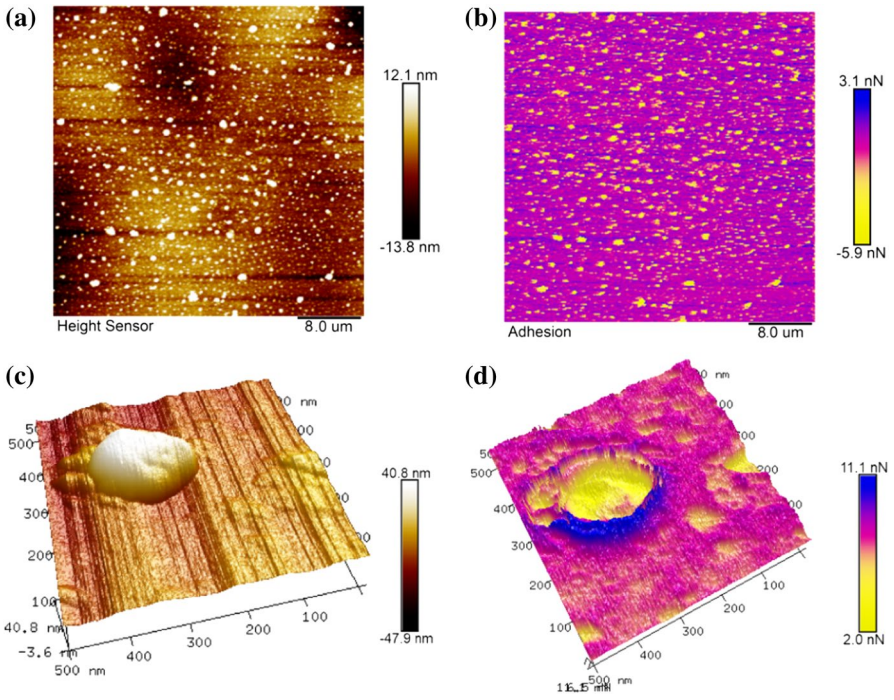

Fig. 9 PeakForce tapping mode in AFM study of Zn/ZnO/Al_2O_3/epoxy composites with 3.0 wt% Zn/ZnO/Al_2O_3 particles. Height image with large scan size (**a**), adhesion image with large scan size (**b**), local height image (**c**), and local adhesion image (**d**)

where k is the thermal conductivity, C_p is the specific heat capacity per unit volume, υ is the phonon velocity and l is the phonon mean free path. For most insulating polymer such as epoxy, the phonon mean free path (l) is extremely small. The reason is that there are lots of defects and grain boundaries in these polymers which may hinder the movement of some phonons. In order to improve the k in epoxy, heat conductive fillers such as Al_2O_3 are usually introduced into epoxy matrix. Figure 10 shows the thermal conductivity of Zn/ZnO/Al_2O_3/epoxy composites as a function of filler loadings. Generally, the thermal conductivity of pure epoxy is low and the value is about 0.14 W m^{-1} K^{-1}. It can be seen that the thermal conductivity remarkably increased with increasing temperature. Meanwhile, the thermal conductivity of the epoxy-containing Zn/ZnO/Al_2O_3 particles was larger than that of pure epoxy. This means that the introduction of core–shell-structured Zn/ZnO/Al_2O_3 particles in epoxy matrix could obviously enhance the thermal conductivity due to the high thermal conductive Al_2O_3 layer coating on the surface of Zn/ZnO particles. In particular, thermal conductivity increased 178% by adding 12.0 wt% of Zn/ZnO/Al_2O_3 particles in epoxy matrix.

As shown in Figs. 11a–c and 12, the dielectric constants of the composites increased obviously after Zn/ZnO/Al_2O_3 fillers embedded in epoxy matrix, while the dielectric loss increased gently (Fig. 12b). It was reported that the core–shell Zn/ZnO/PVDF composites have larger dielectric constant than that of the Zn/PVDF

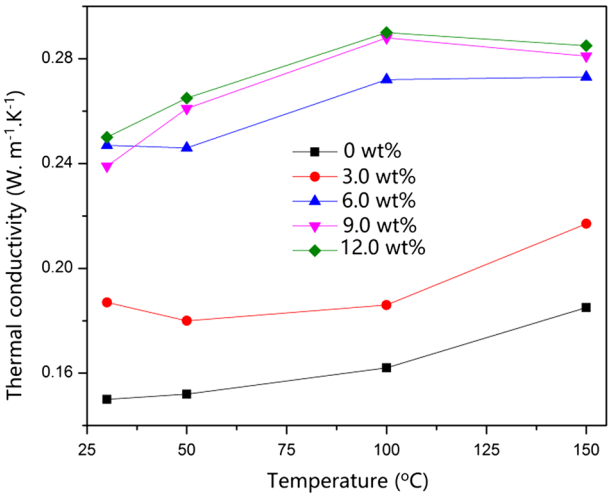

Fig. 10 Thermal conductivity of Zn/ZnO/Al_2O_3/epoxy composites as a function of filler loadings

composites due to the duplex interfacial polarizations induced by metal–semiconductor interface and semiconductor–insulator interface [6]. In this work, the outer layer Al_2O_3 was deposited on the surface of Zn/ZnO, which diminishes the duplex interfacial polarizations and results in a slightly lower dielectric constant compared to the fillers without Al_2O_3 on the surface of Zn/ZnO. On the other hand, the dielectric constant of Al_2O_3 is lower than that of ZnO, which can also cause the decrease in dielectric constant. Nevertheless, the dielectric constant of Zn/ZnO/Al_2O_3/epoxy composites is still high, while the dielectric loss maintains low. As for the dielectric loss, the value of Zn/ZnO/Al_2O_3/epoxy composites presented a modest decrease compared with that of Zn/ZnO/epoxy composites (Fig. 11b, d). The change appeared to be tiny probably due to the incomplete coating of Al_2O_3 over Zn/ZnO particles.

Conclusion

In summary, the core–shell-structured Zn/ZnO particles were prepared by a simple calcination method, and the multilayer core–shell-structured Zn/ZnO/Al_2O_3 particles were synthesized successfully by coating on the surface of Zn/ZnO particles with Al_2O_3 through hydrolysis process. The Zn/ZnO/Al_2O_3/epoxy composites were fabricated, and it can be found that the particles were uniformly distributed in epoxy matrix. Thermal conductivity of Zn/ZnO/Al_2O_3/epoxy composites increased 178% by adding 12.0 wt% of Zn/ZnO/Al_2O_3 particles. The relatively high thermal conductivity and increased dielectric constant in Zn/ZnO/Al_2O_3/epoxy composites are benefitted from the multilayer core–shell structure. The present approach may be extended to the fabrication of advanced polymeric composites with high thermal conductivity and dielectric constant by proper development of multilayer core–shell-structured fillers and selection of polymer matrix. Furthermore, the

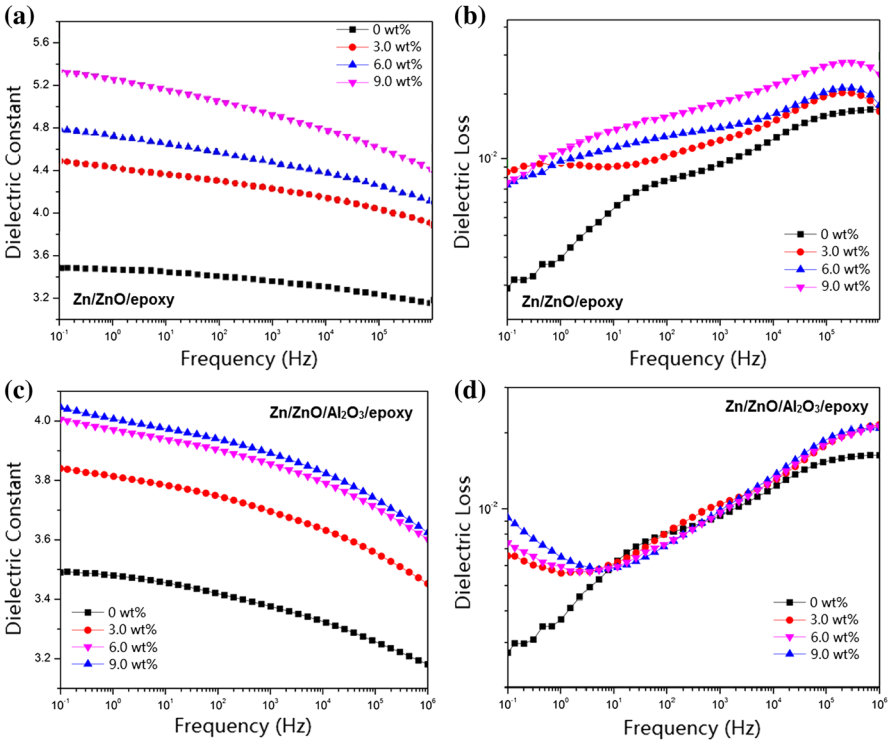

Fig. 11 Dielectric constant (**a**, **c**) and dielectric loss (**b**, **d**) of Zn/ZnO/epoxy composites and Zn/ZnO/Al_2O_3/epoxy composites as a function of filler contents

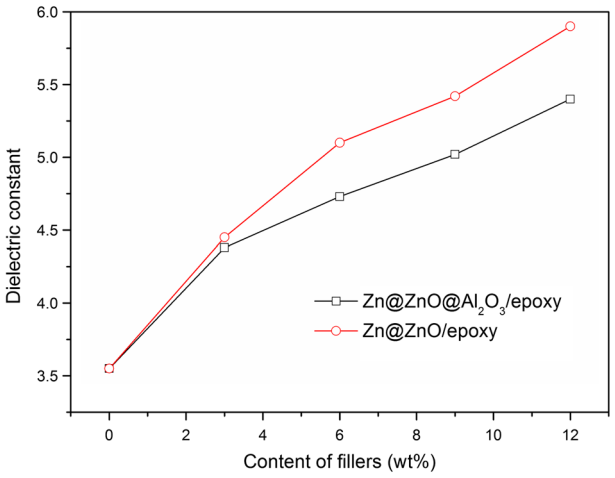

Fig. 12 Evolution of dielectric constant with different fillers

thermal conductivity and the dielectric properties could be further optimized by changing the thickness of Al_2O_3 layer.

Acknowledgements Financial supports from the National Key Research and Development Program of China (Grant No. 2017YFB0903803) and State of Grid (Grant No. SGSNKYOOKJJS1501562) are gratefully acknowledged.

References

1. Wang C, Shieh J (1999) Phosphorus-containing epoxy resin for an electronic application. J Appl Polym Sci 73:353–361. https://doi.org/10.1002/(SICI)1097-4628(19990718)73:3%3c353:AID-APP6%3e3.0.CO;2-V
2. Bo C, Wang J, Zhang F, Qi S (2008) Preparation of silver/carbon fiber/polyaniline microwave absorption composite and its application in epoxy resin. Polym Bull 75:381–393. https://doi.org/10.1007/s00289-017-2035-x
3. Moore A, Shi L (2014) Emerging challenges and materials for thermal management of electronics. Mater Today 17:163–174. https://doi.org/10.1016/j.mattod.2014.04.003
4. Han Z, Fina A (2011) Thermal conductivity of carbon nanotubes and their polymer nanocomposites: a review. Prog Polym Sci 36:914–944. https://doi.org/10.1016/j.progpolymsci.2010.11.004
5. Psarras G, Manolakaki E, Tsangaris G (2003) Dielectric dispersion and AC conductivity in-iron particles loaded-polymer composites. Compos A 34:1187–1198. https://doi.org/10.1016/j.compositesa.2003.08.002
6. Zhang Y, Wang Y, Deng Y, Li M, Bai J (2012) Enhanced dielectric properties of ferroelectric polymer composites induced by metal-semiconductor Zn–ZnO core–shell structure. ACS Appl Mater Interfaces 4:65–68. https://doi.org/10.1021/am2016156
7. Zhou T, Zha J, Hou Y, Wang D, Zhao J, Dang Z (2011) Surface-functionalized MWNTs with emeraldine base: preparation and improving dielectric properties of polymer nanocomposites. ACS Appl Mater Interfaces 3:4557–4560. https://doi.org/10.1021/am201454e
8. Liu Y, Shen Y, Song Y, Nan C, Lin Y, Yang X (2011) Carbon nanotube array/polymer core/shell structured composites with high dielectric permittivity, low dielectric loss, and large energy density. Adv Mater 23:5104–5108. https://doi.org/10.1002/adma.201102079
9. Shen Y, Lin Y, Li M, Nan C (2010) High dielectric performance of polymer composite films induced by a percolating interparticle barrier layer. Adv Mater 19:1418–1422. https://doi.org/10.1002/adma.200602097
10. Thomassin J, Huynen I, Jerome R, Detrembleur C (2010) Functionalized polypropylenes as efficient dispersing agents for carbon nanotubes in a polypropylene matrix; application to electromagnetic interference (EMI) absorber materials. Polymer 51:115–121. https://doi.org/10.1016/j.polymer.2009.11.012
11. Zhou J, Jiang Y, Wu G, Wu W, Wang Y, Wu K, Cheng Y (2017) Investigation of dielectric and thermal conductive properties of epoxy resins modified by core–shell structured PS@SiO_2. Compos A 97:76–82. https://doi.org/10.1016/j.compositesa.2017.03.005
12. Zhou Y, Yao Y, Chen C, Moon K, Wang H, Wong C (2014) The use of polyimide-modified aluminum nitride fillers in AlN@PI/Epoxy composites with enhanced thermal conductivity for electronic encapsulation. Sci Rep 4(4779):1–6. https://doi.org/10.1038/srep04779
13. He F, Lau S, Chan H, Fan J (2009) High dielectric permittivity and low percolation threshold in nanocomposites based on poly(vinylidene fluoride) and exfoliated graphite nanoplates. Adv Mater 21:710–715. https://doi.org/10.1002/adma.200801758
14. Dang Z, You S, Zha J, Song H, Li S (2010) Effect of shell-layer thickness on dielectric properties in Ag@TiO_2 core@shell nanoparticles filled ferroelectric poly(vinylidene fluoride) composites. Phys Status Solidi A 207:739–742. https://doi.org/10.1002/pssa.200925471
15. Zhu J, Wei S, Ryu J, Sun L, Luo Z, Guo Z (2010) Magnetic epoxy resin nanocomposites reinforced with core–shell structured Fe@FeO nanoparticles: fabrication and property analysis. ACS Appl Mater Interfaces 2:2100–2107. https://doi.org/10.1021/am100361h

16. Shi Y, Perterson S, Sogah D (2007) Surfactant-free method for the synthesis of poly(vinyl acetate) masterbatch nanocomposites as a route to ethylene vinyl acetate/silicate nanocomposites. Chem Mater 19:1552–1564. https://doi.org/10.1021/cm060593y
17. Pan Y, Xu Y, An L, Lu H, Yang Y, Chen W, Nutt S (2008) Hybrid network structure and mechanical properties of rodlike silicate/cyanate ester nanocomposites. Macromolecules 41:9245–9259. https://doi.org/10.1021/ma800819s
18. Zhu B, Wang J, Zheng H, Ma J, Wu J, Gan Z, Liu J (2017) Thermal conductivity and dielectric properties of immiscible LDPE/epoxy blend filled with hybrid filler consisting of HGM and nitride particle. J Alloy Compd 15:499–507. https://doi.org/10.1016/j.jallcom.2017.01.182